Energetic Analysis of Pentagon Road Intermediates of C_{60}-Buckminsterfullerene Formation

Kevin R. Bates and Gustavo E. Scuseria*

Chemistry Department, Rice Quantum Institute, and Center for Nanoscale Science and Technology, 6100 Main Street, MS 60, Rice University, Houston, Texas 77005-1892

Received: December 9, 1996; In Final Form: January 29, 1997[⊗]

We report an energetic analysis of the principal intermediates of the pentagon road (PR) scheme for formation of C_{60}-buckminsterfullerene. All calculations were initially performed using the tight-binding semiempirical method. For selected cases, more rigorous 3-21G/HF and 3-21G/B3LYP calculations were carried out. The first part of this study includes an energetic comparison between the 30-, 40-, and 50-atom PR intermediates and a representative group of 30-, 40-, and 50-atom carbon clusters. While C_{30} PR is higher in energy than a large variety of graphene sheets and fullerenes, C_{40} PR and C_{50} PR are considerably lower in energy than many other isomers; only fullerenes are more stable. Additionally, we examine a plausible mechanism by which C_{50} PR rearranges to form a C_{50} cage with D_{5h} symmetry. Because of its large energy barrier, this process is unlikely to affect the C_{60} growth mechanism.

Introduction

C_{60}-buckminsterfullerene (BF) was first detected as a product arising from laser-vaporized graphite.[1] Mass spectrometry and the recently developed technique of ion chromatography[2] give a large amount of information on carbon species present following graphite vaporization. Many schemes of fullerene formation draw from this growing source of data.[3−8] A well-known mechanism for the formation of C_{60} BF, dubbed the pentagon road (PR),[4] explains fullerene formation by imposing the constraint that developing clusters minimize their number of dangling bonds by incorporating a maximal number of nonabutting pentagonal rings. Some of the key intermediates of the PR mechanism are shown in Figure 1A. For the purpose of this work, we assume that C_{20} PR goes to C_{60} BF by stepwise addition of C_2 fragments along the rim of the growing carbon cluster. The portion of this mechanism going from C_{20} PR to C_{30} PR is outlined in Figure 1B. Previous theoretical studies were carried out to determine the energetics underlying C_2 addition and other types of annealing and fragmentation processes for various fullerene systems.[9,10]

The PR mechanism contains several advantageous features. First, many atoms on the cluster rim make up armchair edges, thus minimizing the number of dangling bonds. Furthermore, these intermediates avoid some bonding patterns that are energetically unfavorable, such as adjacent five-membered carbon rings. Issues concerning energetic penalties arising from dangling bonds and curvature strain for similar carbon systems have recently been discussed elsewhere.[11]

Theoretical analysis may reveal important information about the stability of individual PR structures and the overall feasibility of the mechanism. In this study, we perform tight-binding calculations followed by high-quality *ab initio* calculations to determine the energetics of important intermediates predicted by the PR scheme of fullerene growth. In addition, we investigate a mechanism going from C_{50} PR to the C_{50} cage with D_{5h} symmetry. This mechanism may represent an important divergent path from the PR.

Computational Details

Calculations were initially performed using the semiempirical tight-binding (TB) potential for carbon.[12] Properties of the tight-binding potential and functional form are discussed thoroughly elsewhere.[12,13] These calculations were compared with more rigorous calculations using the 3-21G basis set with Hartee−Fock (HF) and Becke's three-parameter hybrid method using the Lee, Yang, and Parr correlational functional (B3LYP).[14,15] All calculations were carried out using a development version of the GAUSSIAN suite of programs.[16] All TB energy values quoted in this paper correspond to molecules with geometries fully optimized by a TB conjugate-gradient scheme. HF and B3LYP energy values were obtained at molecular geometries fully optimized at the 3-21G/HF level of theory.

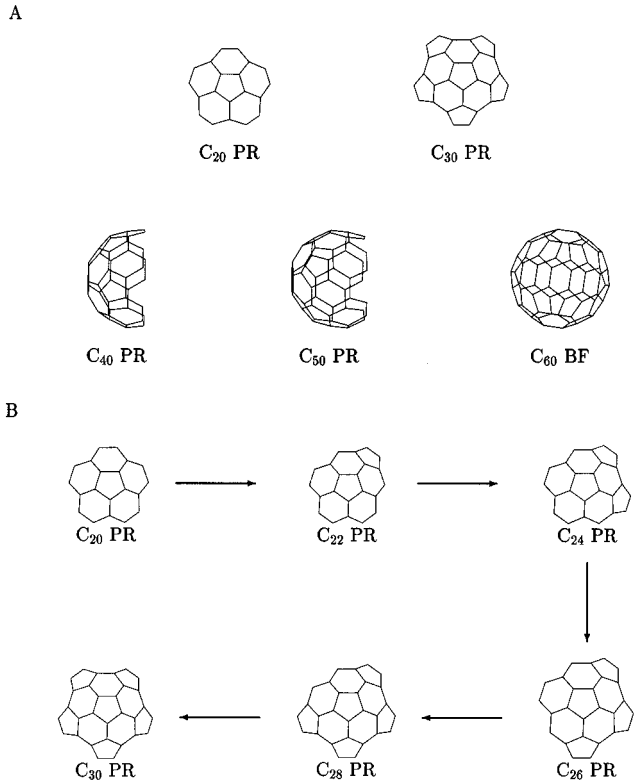

Figure 1. Structures of pentagon road intermediates.

Results

To establish an overall picture of the energetics of the PR mechanism, we carried out TB and 3-21G/HF calculations on

[⊗] Abstract published in *Advance ACS Abstracts,* March 15, 1997.

S1089-5639(96)04021-2 CCC: $14.00 © 1997 American Chemical Society

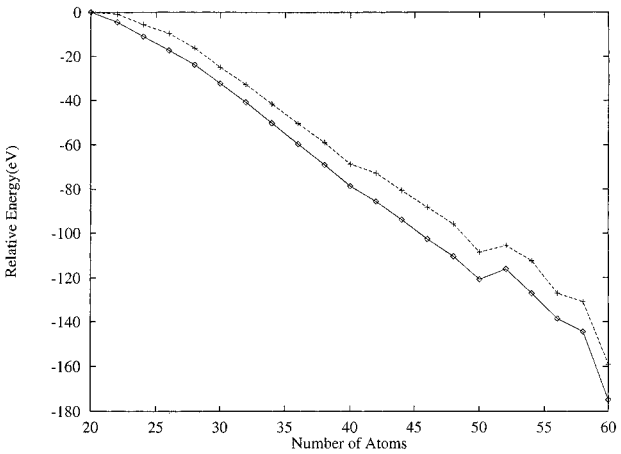

Figure 2. TB (dashed line) and HF (solid line) energies of the reactions C_{60-2m} PR + m*C_2 (m = 0−20), plotted as a function of the number of atoms in each molecule.

TABLE 1: Comparison of the Energies (eV) of Various 30-Atom Carbon Isomers Relative to C_{30} PR (Entry A); See Also Figure 3

molecule	tight-binding[a]	3-21G/HF[b]	3-21G/B3LYP[b]
A	0.0	0.0	0.0
B	−8.9	−11.3	−11.3
C	−7.1	−8.3	−8.9
D	−5.4	−7.3	−6.5
E	−4.4	−6.5	−5.7
F	−4.7	−4.4	−3.5
G	−3.6	−2.1	−1.1
H	−2.0	−0.5	1.4
I	−2.0	0.4	1.9
J	−3.4		
K	−2.0		
L	0.5		
M	0.9		
N	2.4		
O	10.6		

[a] Tight-binding optimized geometry. [b] 3-21G/HF optimized geometry.

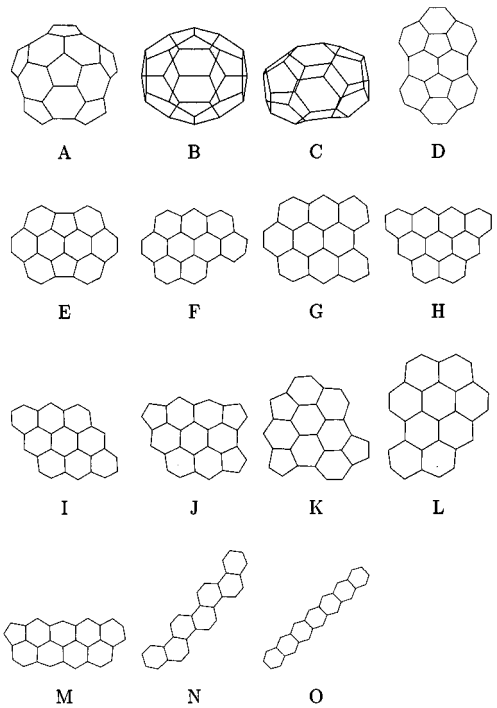

Figure 3. Structures referred to in "molecule" entry of Table 1.

intermediates from C_{20} PR to C_{60} BF. In Figure 2, the energies of the reactions C_{60-2m} PR + mC_2 (m = 0−20) are plotted as a function of the number of atoms in each PR cluster. The steady decrease in energy with growing size of the PR intermediates clearly shows that the PR mechanism is energetically favorable as a whole. However, a signifigant energy barrier is seen for the reaction of C_{50} PR and C_2 to yield C_{52} PR. We predict the magnitude of this barrier to be greater than 1.8 and 3.0 eV, using TB and 3-21G/HF methods, respectively. The signifigance of this energy barrier will be discussed in more detail below.

Next, we examined the stability of the 30-, 40-, and 50-atom PR intermediates as constrasted with other isomers. Results obtained for carbon chains, rings, and cycloadducts[7] are

TABLE 2: Comparison of the Energies (eV) of Various 40-Atom Carbon Isomers Relative to C_{40} PR (A); See Also Figure 4

molecule	tight-binding[a]	3-21G/HF[b]	3-21G/B3LYP[b]
A	0.0	0.0	0.0
B	−1.9	−1.2	−1.9
C	−0.8	0.4	−0.5
D	1.2	1.8	1.6
E	0.3	2.6	1.3
F	3.6	3.0	3.9
G	3.3	8.1	8.4
H	4.1		
I	6.3		
J	9.2		
K	9.6		
L	11.6		
M	11.7		
N	12.0		
O	12.3		
P	12.4		
Q	13.7		
R	15.7		

[a] Tight-binding optimized geometry. [b] 3-21G/HF optimized geometry.

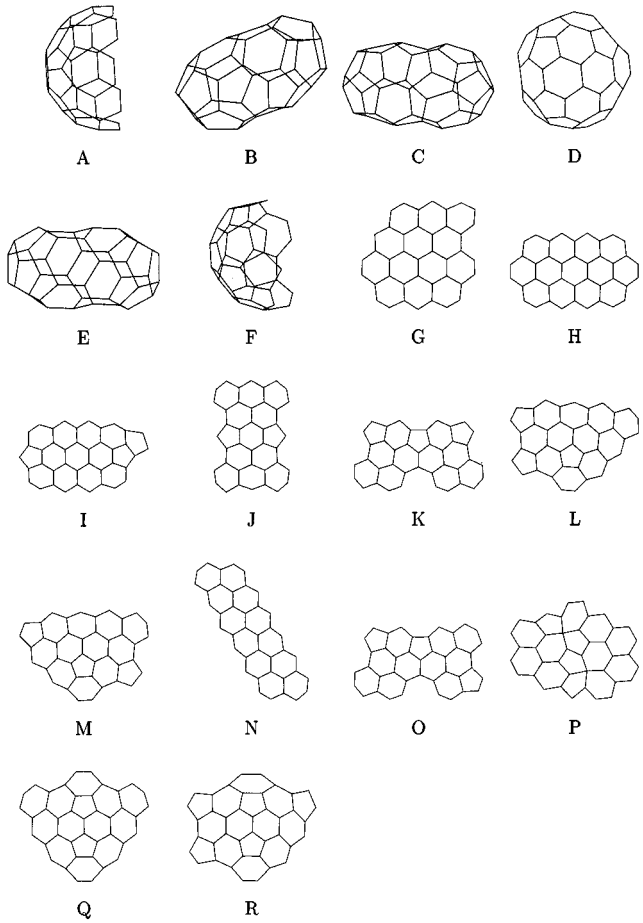

Figure 4. Structures referred to in "molecule" entry of Table 2.

TABLE 3: Comparison of the Energies (eV) of Various 50-Atom Carbon Isomers Relative to C_{50} PR (A); See Also Figure 5

molecule	tight-binding[a]	3-21G/HF[b]	3-21G/B3LYP[b]
A	0.0	0.0	0.0
B	−8.5	−8.2	−7.7
C	7.3	14.2	14.6
D	7.1	14.6	14.9
E	8.6	16.9	18.0
F	8.6		
G	9.2		
H	9.3		
I	10.3		
J	14.4		
K	14.5		
L	18.0		
M	18.3		
N	21.9		
O	23.4		
P	39.5		

[a] Tight-binding optimized geometry. [b] 3-21G/HF optimized geometry.

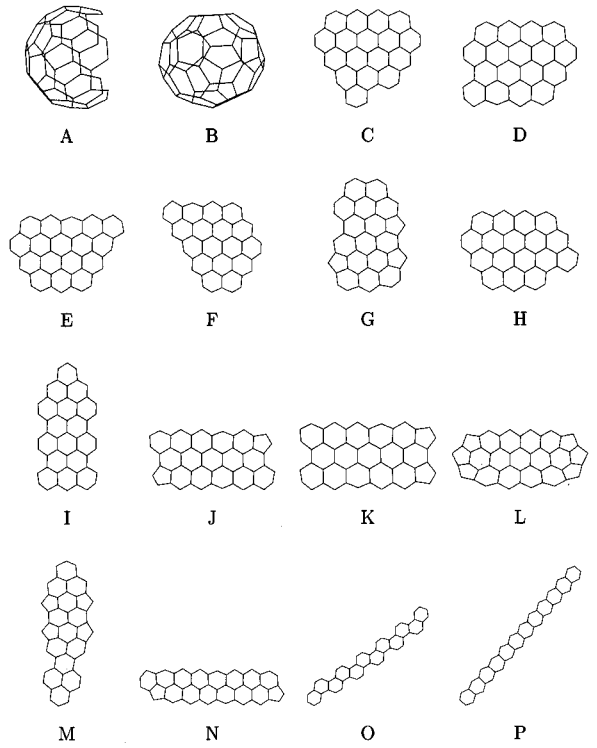

Figure 5. Structures referred to in "molecule" entry of Table 3.

excluded because they are energetically noncompetitive with the PR intermediates. For C_{30}, the monocyclic ring, linear chain, and 4+4 cycloadduct are higher in energy than C_{30} PR as determined by TB calculations by 2.4, 4.7, and 3.3 eV, respectively. Similar results hold for C_{40} and C_{50}. As shown in Table 1, C_{30} PR (Figure 3, entry A, denoted 3A) is higher in energy than a wide variety of molecules in our 30-atom comparison set (3B−3O). Two 30-atom fullerenes (3A,3B) are clearly lower in energy than any of the other 30-atom clusters examined in this study. C_{30} cage with C_{2v} symmetry (3B) is lower in energy than C_{30} PR by 8.9, 11.3, and 11.3 eV, using TB, 3-21G/HF, and 3-21G/B3LYP, respectively. These results are consistent with those found for isomers of C_{24}.[17]

In contrast to C_{30} PR, C_{40} PR (Figure 4A) is much more competitive in energy with molecules in our 40-atom comparison set (4B−4R). As shown in Table 2, C_{40} PR is lower in energy than all tested graphene sheets and fullerenes except the C_{40} fullerene with C_2 symmetry (4B). This fullerene is lower

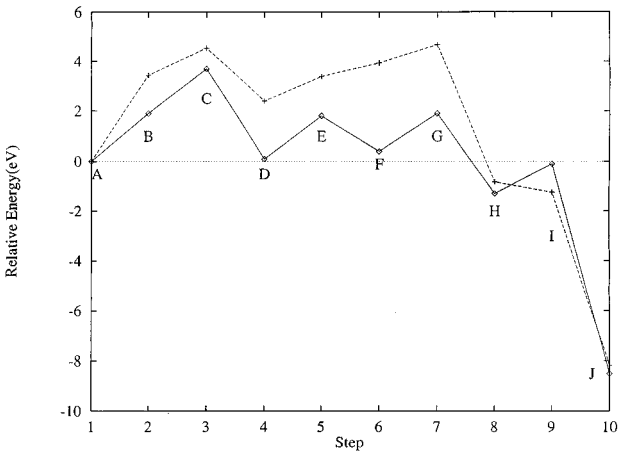

Figure 6. Graph depicting the potential energy surface of one mechanism from C_{50} PR to a C_{50} cage with D_{5h} symmetry. Energies were calculated using TB (dashed) and 3-21G/HF (solid) methods.

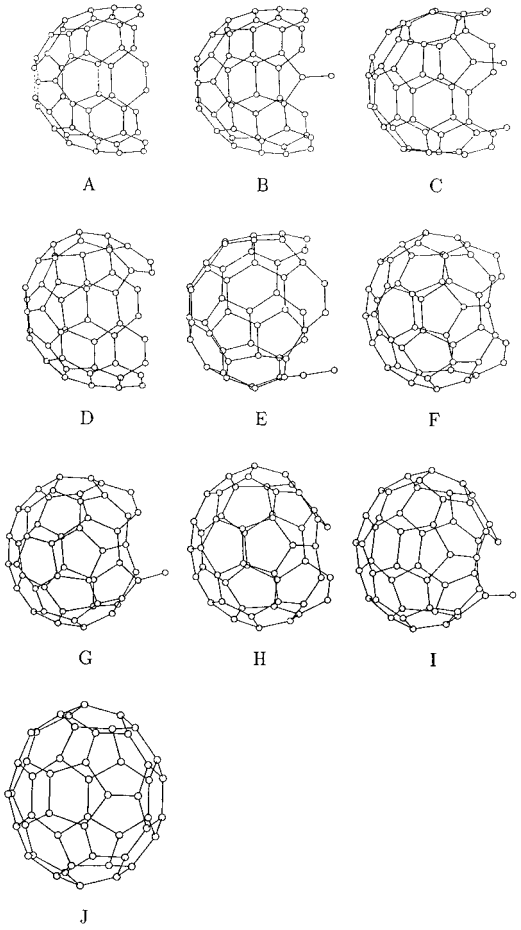

Figure 7. Structures referred to in Figure 6.

in energy than C_{30} PR by 1.9, 1.9, and 1.2 eV, using TB, 3-21G/HF, and 3-21G/B3LYP, respectively.

Results for C_{50} PR (5A) were similar to those obtained for C_{40} PR. As seen in Table 3, the energy difference between the PR structures and chosen graphene sheets continues to increase. Species in Table 3 are depicted in Figure 5. C_{50} with D_{5h} symmetry (5B) is lower in energy than the PR structure by 8.5, 8.2, and 7.7 eV using TB, 3-21G/HF, and 3-21G/B3LYP, respectively.

As shown in Figure 2, the energy of the reaction of C_{50} and C_2 to make C_{52} is energetically uphill. Furthermore, as shown in Table 3, the C_{50} cage with D_{5h} symmetry is considerably lower in energy than C_{50} PR. These results demand further

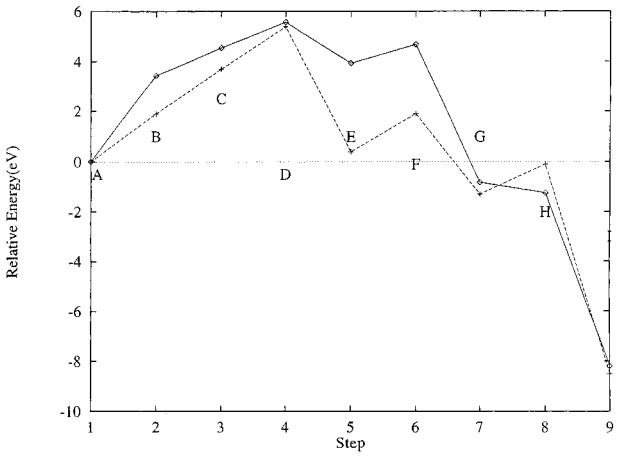

Figure 8. Graph depicting the potential energy surface of a second mechanism from C_{50} PR to a C_{50} cage with D_{5h} symmetry. Energies were calculated using TB (dashed) and 3-21G/HF (solid) methods.

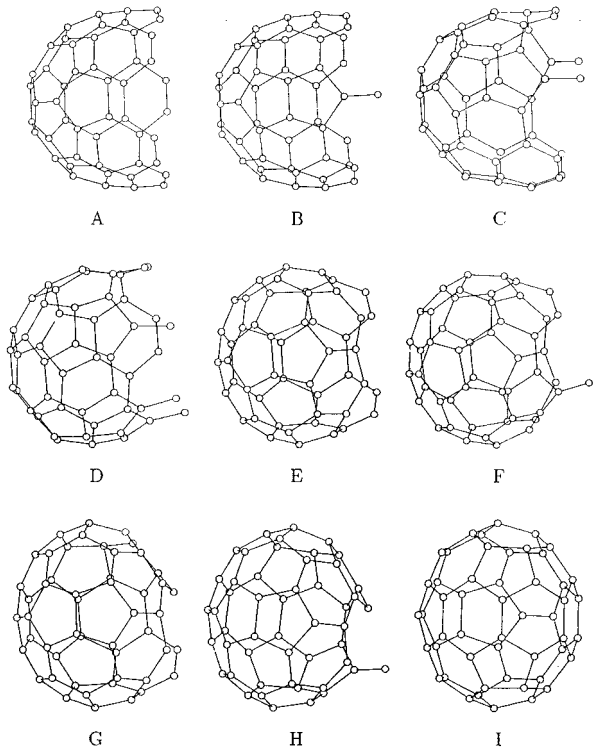

Figure 9. Structures referred to in Figure 8.

investigation of paths from C_{50} PR that diverge from the PR mechanism. One important example of such a pathway is the stepwise conversion of C_{50} PR to C_{50} with D_{5h} symmetry. In Figure 6, we show the potential energy surface of one plausible mechanism for this reaction. Each point on the graph refers to a structure depicted in Figure 7. Mechanism 1 begins by consecutive 1,2-rearrangements of two adjacent armchair edges of C_{50} PR (7A) to produce two C_2 sticks (7B, 7C). These two C_2 sticks bond to form a rim to which additional adjacent C_2 sticks may bond (7D). In the following steps, additional 1,2-rearrangements on adjacent armchair edges result in completion of the rim and closure of C_{50} PR into a C_{50} cage with D_{5h} symmetry. The energy barrier of this mechanism is larger than the highest energy of any one of the intermediates relative to C_{50} PR, which is 4.5 and 3.7 eV using TB and 3-21G/HF, respectively.

Energies for an additional mechanism for the above reaction are shown in Figure 8. Each point on the graph refers to a structure depicted in Figure 9. This mechanism is similar to that for Figure 6, except the first two 1,2-rearrangements occur opposite one another (9B, 9C). This requires that a third 1,2-rearrangement occur (9D) before a rim composed of three bound sticky ends can form (9E). This mechanism then proceeds identically to mechanism 1, resulting in a C_{50} cage with D_{5h} symmetry (9I). The energy barrier of this mechanism is 5.7 and 5.6 eV according to our TB and 3-21G/HF predictions, respectively.

The results of our study provide an energetic evaluation of important intermediates of the pentagon road mechanism for C_{60} BF formation. In contrast with C_{30} PR, which is higher in energy than most 30-atom graphene sheets in our comparison set, C_{40} and C_{50} PR are energetically competitive with a variety of 40- and 50-atom graphene sheets. However, 30-, 40-, and 50-atom fullerenes are lower in energy than each of these PR intermediates. Also, an energy barrier between C_{50} and C_{52} PR suggests the possible existence of alternative mechanisms from C_{50} PR. We examined two such paths from C_{50} PR to a lower energy C_{50} isomer, C_{50} with D_{5h} symmetry. However, we predict that energy barriers for these two mechanisms are too high to be reached at experimental temperatures for high-yield synthesis of C_{60}.

Acknowledgment. This work was supported by the National Science Foundation (CHE-9321297) and the Welch Foundation.

References and Notes

(1) Kroto, H. W.; Heath, J. R.; O'Brien, S. C.; Curl, R. F.; Smalley, R. E. *Nature* **1985**, *318*, 162.
(2) Kemper, P. R.; Bowers, M. T. *J. Am. Soc. Mass Spectrom.* **1990**, *1*, 197.
(3) Kroto, H. W. *Science* **1988**, *242*, 1139.
(4) Smalley, R. E. *Acc. Chem. Res.* **1992**, *25*, 98.
(5) Curl, R. F. *Philos. Trans. R. Soc. London, Ser. A* **1993**, *343*, 19.
(6) Hunter, J.; Fye, J.; Jarrold, M. F. *Science* **1993**, *260*, 784.
(7) Strout, D. L.; Scuseria, G. E. *J. Chem. Phys.* **1996**, *100*, 6492.
(8) Goroff, N. S. *Acc. Chem. Res.* **1996**, *29*, 77.
(9) Murry, R. L.; Strout, D. L.; Odom, G. K.; Scuseria, G. E. *Nature* **1993**, *366*, 665.
(10) Murry, R. L.; Strout, D. L.; Scuseria, G. E. *Int. J. Mass Spectrom. Ion Processes* **1994**, *138*, 113.
(11) Thess, A.; Lee, R.; Nikolaev, P.; Dai, H.; Petit, P.; Robert, J.; Xu, C. H.; Lee, Y. H.; Kim, S. G.; Rinzler, A. G.; Colbert, D. T.; Scuseria, G. E.; Tománek, D.; Fischer, J. E.; Smalley, R. E. *Science* **1996**, *273*, 483.
(12) Xu, C. H.; Wang, C. Z.; Chan, C. T.; Ho, K. H. *J. Phys. Condens. Matter* **1992**, *4*, 6047.
(13) Xu, C. H.; Scuseria, G. E. *Chem. Phys. Lett.* **1996**, *262*, 219.
(14) Becke, A. D. *J. Chem. Phys.* **1993**, *98*, 5648.
(15) Lee, C.; Yang, W.; Parr, R. G. *Phys. Rev. B* **1988**, *37*, 785.
(16) Frisch, M. J.; Trucks, G. W.; Schlegel, H. B.; Scuseria, G. E.; Robb, M. A.; Cheeseman, J. R.; Strain, M. C.; Burant, J. C.; Stratmann, R. E.; Petersson, G. A.; Montgomery, J. A.; Zakrzewski, V. G.; Keith, T.; Raghavachari, K.; Al-Laham, M. A.; Ortiz, J. V.; Foresman, J. B.; Cioslowski, J.; Stefanov, B. B.; Nanayakkara, A.; Challacombe, M.; Peng, C. Y.; Ayala, P. Y.; Chen, W.; Wong, M. W.; Andres, J. L.; Replogle, E. S.; Gomperts, R.; Martin, R. L.; Fox, D. J.; Binkley, J. S.; Defrees, D. J.; Baker, J.; Stewart, J. P.; Gonzalez, C.; Head-Gordon, M.; Gill, P. M. W.; Johnson, B. G.; Pople, J. A. *Gaussian 95*, Development Version (Revision D.2); Gaussian, Inc.: Pittsburgh, PA, 1996.
(17) Raghavachari, K.; Zhang, B.; Pople, J. A.; Johnson, B. J.; Gill, P. M. W. *Chem. Phys. Lett.* **1994**, *220*, 385.